JOURNAL OF BACTERIOLOGY, July 1992, p. 4504–4508
0021-9193/92/134504-05$02.00/0

Vol. 174, No. 13

Immunocytochemical Localization of Glycolytic and Fermentative Enzymes in *Zymomonas mobilis*†

H. C. ALDRICH,[1]* L. McDOWELL,[1] M. DE F. S. BARBOSA,[1] L. P. YOMANO,[1] R. K. SCOPES,[2] AND L. O. INGRAM[1]

Department of Microbiology and Cell Science, University of Florida, Gainesville, Florida 32611-0116,[1] and Centre for Protein and Enzyme Technology, La Trobe University, Bundoora, Victoria, Australia 3083[2]

Received 14 February 1992/Accepted 28 April 1992

Gold-labeled antibodies were used to examine the subcellular locations of 11 glycolytic and fermentative enzymes in *Zymomonas mobilis*. Glucose-fructose oxidoreductase was clearly localized in the periplasmic region. Phosphogluconate lactonase and alcohol dehydrogenase I were concentrated in the cytoplasm near the plasma membrane. The eight remaining enzymes were more evenly distributed within the cytoplasmic matrix. Selected enzyme pairs were labeled on opposite sides of the same thin section to examine the frequency of colocalization. Results from these experiments provide evidence that glyceraldehyde-3-phosphate dehydrogenase, phosphoglycerate kinase, and alcohol dehydrogenase I form an enzyme complex.

The obvious commercial applications of an efficient microbial process for ethanol production have focused *Zymomonas mobilis* research efforts on the enzymes in glycolysis and fermentation (19, 22, 25–27) and on the characterization of the respective genes (5, 9, 10, 15, 18, 20). The spatial arrangement of these enzymes represents a further level of organization which may substantially affect efficiency within these pathways. The development of increasingly effective gold-labeling protocols for transmission electron microscopy has enabled researchers to more precisely seek the cellular locations of enzymes (1, 3, 7, 24). Such an approach is particularly important in prokaryotes, since details of compartmentalization of metabolism are only beginning to emerge. Localization of cellular sites of enzyme activity in both archaea and bacteria has been one of the most exciting areas in which this technique has been employed (3, 17, 21, 24).

As an initial approach to examine protein complexes in *Z. mobilis*, we have used immunocytochemical staining with colloidal gold probes to investigate 12 enzymes which compose the pathways for glycolysis and fermentation. Evidence that these enzymes are not randomly distributed in the cytoplasm and that some of them function as part of a multienzyme complex is presented.

Antibody preparation and specificity. Enzymes were purified to apparent homogeneity essentially as described previously (13, 19, 22, 25–27, 31) and were used to prepare polyclonal antibodies in goats (9) or New Zealand White rabbits (4, 18). All antisera produced a single sharp band in Ouchterlony assays when tested against protein extracts from *Z. mobilis*. Antibodies were purified by caprylic acid extraction, ammonium sulfate precipitation, and adsorption against an acetone powder of *Escherichia coli* according to standard procedures (14).

Specificities of the antisera were examined by Western blotting (immunoblotting) of sodium dodecyl sulfate–12.5% polyacrylamide gels (16) containing *Z. mobilis* protein extracts (Fig. 1). Antibodies to the 12 enzymes stained single dominant bands at the expected molecular weights (4). Antisera against phosphoglycerate mutase (PGM), phosphogluconate lactonase (PGL), and alcohol dehydrogenase II (ADHII) also stained minor bands, each of which appeared slightly smaller than twice the corresponding monomeric size. In the case of ADHII, both bands appear to contain authentic protein since both were also present in recombinant *E. coli* containing the minimal coding region for *adhB*. Several higher-molecular-weight bands were evident with PGL antiserum.

Localization of individual enzymes. *Z. mobilis* CP4 was grown in complex medium containing 10% glucose (18). Log-phase cultures (optical density at 550 nm, 0.8; approximately 250 μg of cells [dry weight] per ml) were chilled (0°C) and fixed for 10 min in cacodylate buffer (pH 7.2) containing 2.5% formaldehyde and 0.5% glutaraldehyde (2). Cells were dehydrated and embedded in Lowicryl K4M with progressive lowering of temperatures (8). Resin was polymerized with UV light (−20°C, 48 h). Sections were supported on Formvar-coated nickel grids, incubated with primary antibody (1 h at 23°C or 16 h at 4°C), washed with phosphate-buffered saline, incubated with secondary antibody carrying 15-nm-diameter gold particles (1 h at 23°C), washed, and poststained with uranyl acetate and lead citrate. Controls

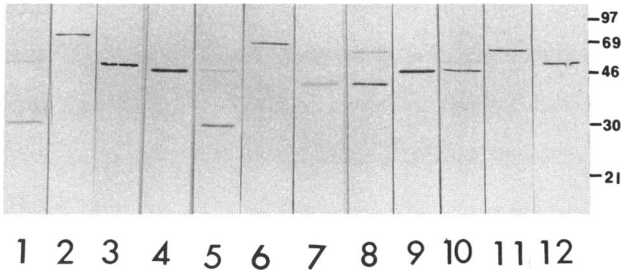

FIG. 1. Western analysis of antibody specificity against sodium dodecyl sulfate-polyacrylamide gels containing soluble *Z. mobilis* proteins. All lanes except lane 1 (7 μg) contained approximately 1 μg of soluble *Z. mobilis* protein. For abbreviations, see Table 1, footnote *a*. Lanes: 1, PGL; 2, PGT; 3, GAPDH; 4, PGK; 5, PGM; 6, PDC; 7, ADHI; 8, ADHII; 9, ENO; 10, GFOR; 11, PYK; 12, GDH (glucose-6-phosphate dehydrogenase). Molecular masses (in kilodaltons) are shown at the right.

* Corresponding author.
† Florida Agricultural Experiment Station publication N-00578.

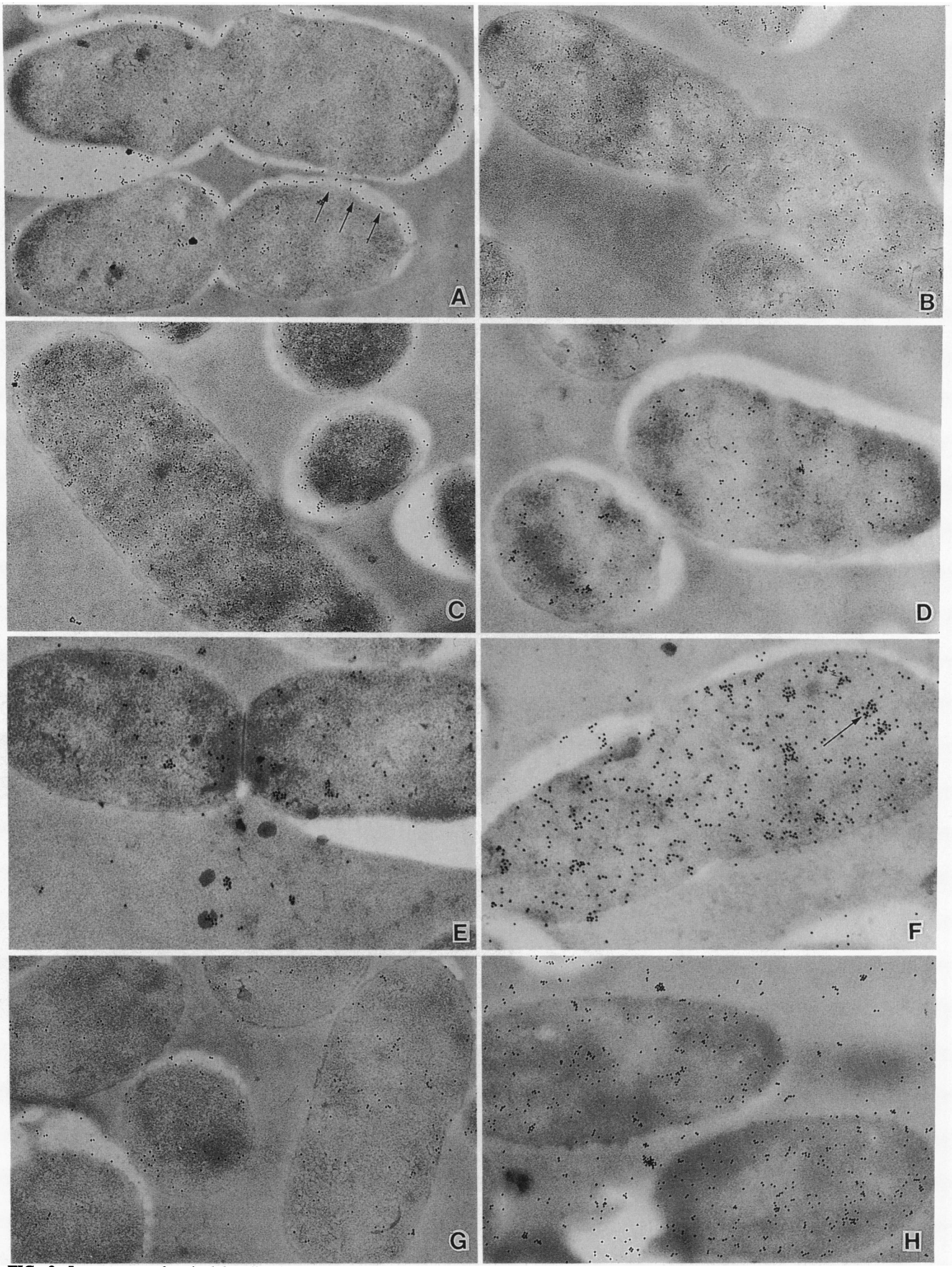

FIG. 2. Immunocytochemical localization of individual glycolytic and fermentative enzymes. Arrows in panel A show the regional localization of PGL in plastic remaining after the cell has pulled away. The arrow in panel F identifies an aggregate of gold particles staining PDC. For abbreviations, see Table 1, footnote *a*. Enzymes and approximate magnifications: panel A, PGL (×19,000); panel B, PGT (×22,000); panel C, GAPDH (×21,000); panel D, PGK (×22,000); panel E, PGM (×27,000); panel F, PDC (×22,000); panel G, ADHI (×21,000); panel H, ADHII (×22,000).

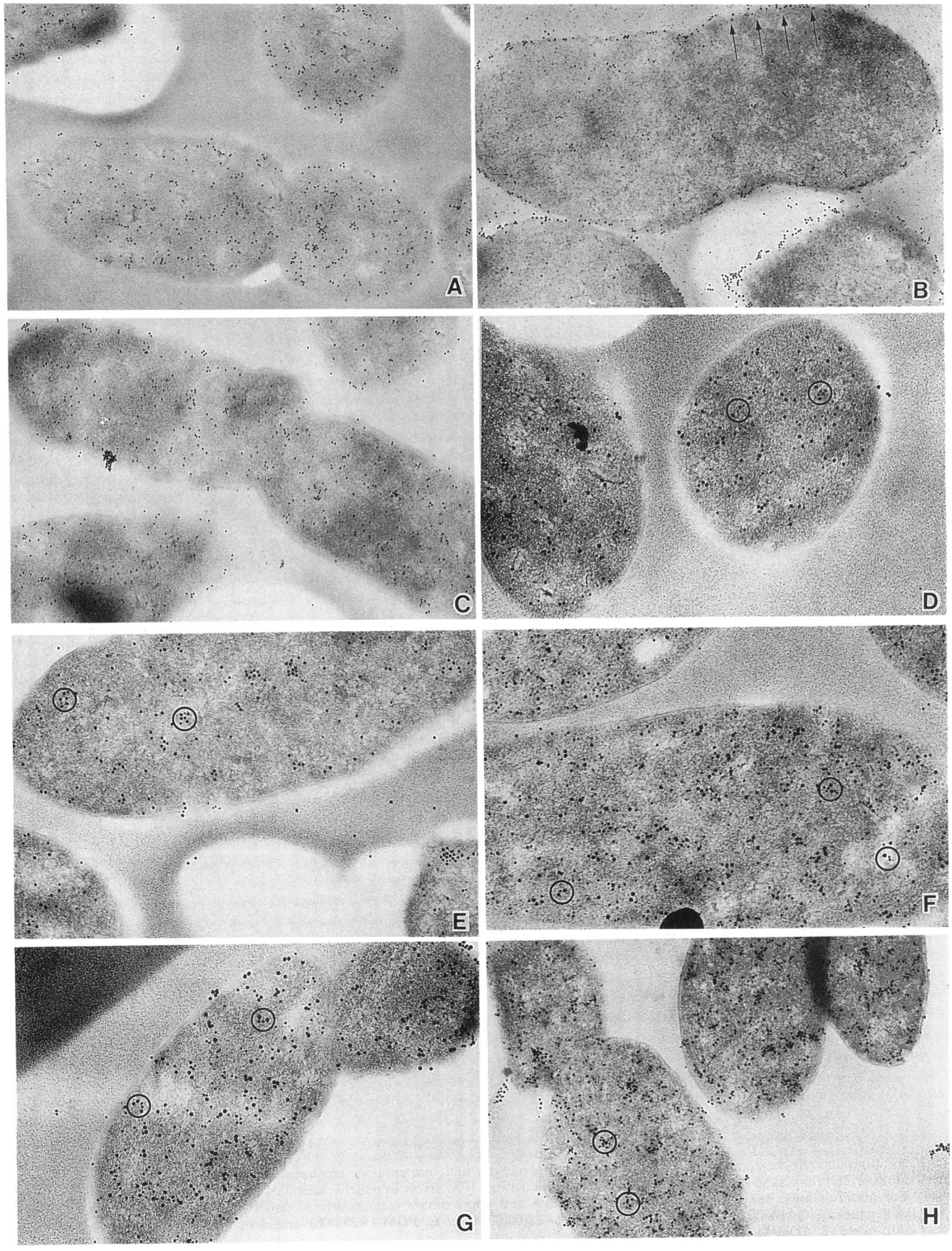
A
B
C
D
E
F
G
H

TABLE 1. Ratios of gold-labeled probe particles which are associated with plasma membrane

Enzyme[a]	Membrane/cytoplasm ratio ± SD (no. of micrographs)[b]	Figure
GFOR	6.7 ± 0.2 (14)	3B
PGL	2.4 ± 0.1 (3)	2A
ADHI	1.3 ± 0.1 (6)	2G
ADHII	0.8 ± 0.1 (3)	2H
PGM	0.7 ± 0.1 (3)	2E
PYK	0.6 ± 0.1 (4)	3C
PDC	0.5 ± 0.1 (4)	2F
GAPDH	0.5 ± 0.1 (3)	2C
ENO	0.5[c] (2)	3A
PGK	0.5[c] (2)	2D
PGT	0.4 ± 0.1 (3)	2B

[a]Abbreviations: GFOR, glucose-fructose oxidoreductase; PGL, phosphogluconate lactonase; ADHI and ADHII, alcohol dehydrogenases I and II, respectively; PGM, phosphoglycerate mutase; PYK, pyruvate kinase; PDC, pyruvate decarboxylase; GAPDH, glyceraldehyde-3-phosphate dehydrogenase; ENO, enolase; PGK, phosphoglycerate kinase; PGT, 6-phosphogluconate dehydratase.

[b]Sections were stained with immunogold to localize individual enzymes. Gold particles were counted within the same number of 0.1-μm^2 areas surrounding the plasma membrane as the number of areas in the cytoplasm, using paper masks. These were totaled for each micrograph (3 to 10 cells per micrograph) and expressed as a ratio. These ratios were averaged (3 to 14 micrographs) for each enzyme to calculate the standard deviation. The membrane/cytoplasmic ratio for randomly distributed cytoplasmic enzymes would be expected to be around 0.5 because of the improbability of such enzymes being localized in the area outside of the plasma membrane.

[c]Standard deviation not determined.

TABLE 2. Enzyme colocalization: percentage of small gold particles which lie within 20 nm of large gold particles

Enzyme[a] (gold probe diam in nm)	% Colocalized particles ± SD (no. of micrographs)[b]	Random association[c]	Figure
ADHI (10) + GAPDH (15)	79 ± 2 (6)	14	3D
GAPDH (10) + PGK (15)	51 ± 1 (6)	17	3E
ADHII (10) + PDC (15)	40 ± 1 (4)	13	3F
ADHII (10) + GAPDH (15)	38 ± 1 (6)	12	3G
PGT (10) + PGM (15)	35 ± 1 (6)	9	3H

[a]For abbreviations, see Table 1, footnote *a*.

[b]Sections were stained with immunogold to localize one enzyme on either side of thin sections first with the large gold probe and then with the small gold probe. The total number of small gold particles and the number of small gold particles within 20 nm of a large gold particle were counted. These were summed for each micrograph (3 to 10 cells per micrograph) and expressed as a percentage of small gold particles colocalized with large gold particles. Percentages from four to six micrographs were averaged to calculate the standard deviation.

[c]The percentages of association expected from random events were calculated on the basis of the number of particles per unit area.

were incubated with preimmune serum instead of primary antibody and exposed to secondary antibody alone. Sections were photographed with a JEOL 100-CX or a Hitachi HU-11E transmission electron microscope.

All enzymes except glucose-fructose oxidoreductase (GFOR) were more abundant in the cytoplasmic matrix between the lighter, nucleic acid-rich regions (Fig. 2 and 3A through C). Clusters of gold particles were observed with all enzymes even though gold-labeled antibodies had been centrifuged to eliminate aggregates immediately prior to use. These clusters were particularly evident with pyruvate decarboxylase (PDC) and may represent associations between molecules in the cytoplasm (Fig. 2F). No binding of antiserum to glucose 6-phosphate dehydrogenase was observed in thin sections even at a low dilution (1:10) despite the effectiveness of this antibody in Western blots.

GFOR was localized in the periplasmic region, in agreement with previous studies (17). This localization is further supported by the presence of a leader sequence in the coding region that is cleaved upon export (unpublished data). Two enzymes, PGL (Fig. 2A) and ADHI (Fig. 2G), appeared more abundant near the plasma membrane. This localization was confirmed quantitatively by measuring the distribution of label. Paper templates were constructed, and their dimensions corresponded to the width of the membrane (10 nm) plus two antibody diameters (24) on each side (4 × 8 nm) plus the diameters of two gold particles (2 × 15 nm), or 72 nm in total width by a length of 1.4 μm (approximate area, 0.1 μm^2). By using these templates as masks, gold particles within open areas near the plasma membrane and in the cytoplasmic matrix were counted (Table 1). The high membrane/cytoplasm ratio for GFOR, PGL, and ADHI confirmed this membrane localization.

Colocalization of selected enzymes. In dual-label experiments, thin sections supported on uncoated grids were exposed to primary antibody and then to secondary antibody labeled with 15-nm-diameter gold particles. Grids were then inverted to expose the opposite side to a second primary antibody and then to secondary antibody containing 10-nm-diameter gold particles. The number of small gold particles located within 20 nm of large gold particles was determined by counting and was expressed as a percentage of the total small particles (Table 2). A pronounced association was observed for ADHI with glyceraldehyde-3-phosphate dehydrogenase (GAPDH) (79%; Fig. 3D) and for GAPDH with phosphoglycerate kinase (PGK) (51%; Fig. 3E) compared with three other combinations. The associations of ADHII with GAPDH (Fig. 3G), 6-phosphogluconate dehydratase (PGT) with PGM (Fig. 3H), and ADHII with PDC (Fig. 3F) ranged from 35 to 40%. With this procedure, false association due to random labeling within 20 nm would also be expected. However, the predicted random colocalization based on observed particle densities per unit area was much lower than the observed associations for each enzyme pair.

The most pronounced associations were between ADHI, GAPDH, and PGK. Previous studies have provided in vitro kinetic evidence for functional complexes between GAPDH and PGK from muscle tissues (6, 22, 30), but similar work in

FIG. 3. Immunocytochemical localization (A through C) and colocalization (D through H) of individual glycolytic and fermentative enzymes. Colabeling experiments are summarized in Table 2. Sections were stained on one side with primary antibody and secondary antibody carrying 15-nm-diameter gold particles. The other side was stained with a different primary antibody and secondary antibody carrying 10-nm-diameter gold particles. Arrows in panel B illustrate the localization of GFOR antibody near the surface of the cell. Circles in panels D through H contain large and small gold particles which appear to colocalize. For abbreviations, see Table 1, footnote *a*. Enzymes and approximate magnifications: panel A, ENO (×21,000); panel B, GFOR (×22,000); panel C, PYK (×22,000); panel D, GAPDH plus ADHI (×44,000); panel E, PGK plus GAPDH (×44,000); panel F, PDC plus ADHII (×33,000); panel G, GAPDH plus ADHII (×33,000); panel H, PGM plus PGT (×44,000).

Z. mobilis has not been performed. Analogous studies with muscle and yeast enzymes have also provided kinetic evidence for associations between GAPDH and fermentative enzymes, such as lactate dehydrogenase and alcohol dehydrogenase, which oxidize NADH (6, 29, 30). During evolution, a pronounced chirality has been conserved for NADH-linked and NADPH-linked dehydrogenases with regard to the hydrogen being transferred (23, 28, 30). NADH can be regarded as having two surfaces for enzyme binding. In all cases examined, enzymes which generate NADH, such as GAPDH, bind one surface while fermentative enzymes which oxidize NADH, such as alcohol dehydrogenases and lactate dehydrogenases, bind the complementary face. *Z. mobilis* ADHII has been demonstrated to bind the predicted face of NADH (11). Although the chirality of *Z. mobilis* GAPDH and ADHI has not been reported, the high degree of amino acid homology between these enzymes (10, 15) and the corresponding yeast enzymes provides strong evidence for the predicted chirality.

In *E. coli*, large complexes involving most of the glycolytic enzymes have been reported (12). Although a limited number of associations have been investigated in *Z. mobilis*, the observed associations between ADHI, GAPDH, and PGK may represent part of a similar large complex with additional glycolytic enzymes in *Z. mobilis*.

This research was supported in part by grant FG05-86ER3574 from the DOE Office of Basic Energy Science and by grants from the Australian Research Council and the Australian Universities International Development Plan.

REFERENCES

1. **Acker, G.** 1988. Immunoelectron microscopy of surface antigens. Methods Microbiol. **20:**147–174.
2. **Aldrich, H. C., D. B. Beimborn, and P. Schönheit.** 1987. Creation of artifactual internal membranes during fixation of *Methanobacterium thermoautotrophicum*. Can. J. Microbiol. **33:** 844–849.
3. **Aldrich, H. C., D. B. Beimborn, and P. Schönheit.** 1987. Immunocytochemical localization of methyl-coenzyme M reductase in *Methanobacterium thermoautotrophicum*. Arch. Microbiol. **147:**190–194.
4. **An, H., R. K. Scopes, M. Rodriguez, K. F. Keshav, and L. O. Ingram.** 1991. Gel electrophoretic analysis of *Zymomonas mobilis* glycolytic and fermentative enzymes: identification of alcohol dehydrogenase II as a stress protein. J. Bacteriol. **173:**5975–5982.
5. **Barnell, W. O., K. C. Yi, and T. Conway.** 1990. Sequence and genetic organization of a *Zymomonas mobilis* gene cluster that encodes several enzymes of glucose metabolism. J. Bacteriol. **172:**7227–7240.
6. **Batke, J.** 1989. Channeling of glycolytic intermediates by temporary, stationary bienzyme complexes is probable *in vivo*. Trends Biochem. Sci. **14:**481–482.
7. **Bendayan, M.** 1984. Protein A-gold electron microscopic immunocytochemistry: methods, applications and limitations. J. Electron Microsc. Tech. **1:**243–270.
8. **Carlemalm, E., and W. Villiger.** 1989. Low temperature embedding, p. 29–45. *In* G. Bullock and P. Petrusz (ed.), Techniques in immunocytochemistry, vol. 4. Academic Press, Inc., New York.
9. **Conway, T., Y. A. Osman, J. I. Konnan, E. M. Hoffmann, and L. O. Ingram.** 1987. Promoter and nucleotide sequences of the *Zymomonas mobilis* pyruvate decarboxylase. J. Bacteriol. **169:** 949–954.
10. **Eddy, C. K., K. F. Keshav, H. An, E. A. Utt, J. P. Mejia, and L. O. Ingram.** 1991. Segmental message stabilization as a mechanism for differential expression from the *Zymomonas mobilis gap* operon. J. Bacteriol. **173:**245–254.
11. **Glasfeld, A., and S. A. Benner.** 1989. The stereospecificity of the ferrous-ion-dependent alcohol dehydrogenase from *Zymomonas mobilis*. Eur. J. Biochem. **180:**373–375.
12. **Gorringe, D. M., and V. Moses.** 1980. Organization of the glycolytic enzymes in *Escherichia coli*. Int. J. Biol. Macromol. **2:**161–173.
13. **Hardman, M. J., and R. K. Scopes.** 1988. The kinetics of glucose-fructose oxidoreductase from *Zymomonas mobilis*. Eur. J. Biochem. **173:**203–209.
14. **Harlow, E., and D. Lane.** 1988. Antibodies. A laboratory manual. Cold Spring Harbor Laboratory, Cold Spring Harbor, N.Y.
15. **Keshav, K. F., L. P. Yomano, H. An, and L. O. Ingram.** 1990. Cloning of the *Zymomonas mobilis* structural gene encoding alcohol dehydrogenase I (*adhA*): sequence comparison and expression in *Escherichia coli*. J. Bacteriol. **172:**2491–2497.
16. **Laemmli, U. K.** 1970. Cleavage of structural proteins during the assembly of the head of bacteriophage T4. Nature (London) **227:**680–685.
17. **Loos, H., M. Voller, B. Rehr, Y.-D. Stierhof, H. Sahm, and G. A. Springer.** 1991. Localisation of the glucose-fructose oxidoreductase in wild type and overproducing strains of *Zymomonas mobilis*. FEMS Microbiol. Lett. **84:**211–216.
18. **Mackenzie, K. F., C. K. Eddy, and L. O. Ingram.** 1989. Modulation of alcohol dehydrogenase isoenzyme levels in *Zymomonas mobilis* by iron and zinc. J. Bacteriol. **171:**1063–1067.
19. **Neale, A. D., R. K. Scopes, J. M. Kelly, and R. E. H. Wettenhall.** 1986. The two alcohol dehydrogenases of *Zymomonas mobilis*: purification by differential dye ligand chromatography, molecular characterization and physiological role. Eur. J. Biochem. **154:**119–124.
20. **Neale, A. D., R. K. Scopes, R. E. H. Wettenhall, and N. J. Hoogenraad.** 1987. Nucleotide sequence of the pyruvate decarboxylase gene from *Zymomonas mobilis*. Nucleic Acids Res. **15:**1753–1761.
21. **Ossmer, R., T. Mund, P. L. Hartzell, U. Konheiser, G. W. Kohring, A. Klein, R. S. Wolfe, G. Gottschalk, and F. Mayer.** 1986. Immunocytochemical localization of component C of the methylreductase system in *Methanococcus voltae* and *Methanobacterium thermoautotrophicum*. Proc. Natl. Acad. Sci. USA **83:**5789–5792.
22. **Pawluk, K. A., R. K. Scopes, and K. Griffiths-Smith.** 1986. Isolation and properties of the glycolytic enzymes from *Zymomonas mobilis*. The five enzymes from glyceraldehyde-3-phosphate through pyruvate kinase. Biochem. J. **238:**275–281.
23. **Popjak, G.** 1970. Stereospecificity of enzymatic reactions, p. 115–215. *In* P. D. Boyer (ed.), The enzymes, vol. III. Academic Press, Inc., New York.
24. **Rohde, M., H. Gerberding, T. Mund, and G.-W. Kohring.** 1988. Immunoelectron microscopic localization of bacterial enzymes: pre- and post-embedding labelling techniques on resin-embedded samples. Methods Microbiol. **20:**175–210.
25. **Scopes, R. K.** 1985. 6-Phosphogluconolactonase from *Zymomonas mobilis*. FEBS Lett. **193:**185–188.
26. **Scopes, R. K., and K. Griffiths-Smith.** 1984. Use of differential dye-ligand chromatography with affinity elution for enzyme purification: 6-phosphogluconate dehydratase from *Zymomonas mobilis*. Anal. Biochem. **136:**530–534.
27. **Scopes, R. K., V. Testolin, A. Stoter, K. Griffiths-Smith, and E. M. Algar.** 1985. Simultaneous purification and characterization of glucokinase, fructokinase and glucose-6-phosphate dehydrogenase from *Zymomonas mobilis*. Biochem. J. **228:**627–634.
28. **Srere, P. A.** 1987. Complexes of sequential metabolic enzymes. Annu. Rev. Biochem. **56:**89–124.
29. **Srivastava, D. K., and S. A. Bernhard.** 1984. Direct transfer of NADH from glyceraldehyde 3-phosphate dehydrogenase to liver alcohol dehydrogenase. Biochemistry **23:**4338–4345.
30. **Srivastava, D. K., and S. A. Bernhard.** 1986. Metabolite transfer via enzyme-enzyme complexes. Science **234:**1081–1086.
31. **Zachariou, M., and R. K. Scopes.** 1986. Glucose-fructose oxidoreductase, a new enzyme isolated from *Zymomonas mobilis* that is responsible for sorbitol production. J. Bacteriol. **167:**863–869.